International Journal of Research and Review
[Indexed, Peer-Reviewed Journal]
Volume 13; Issue: 6; June 2026
Website: www.ijrrjournal.com
Research Paper *E-ISSN: 2349-9788; P-ISSN: 2454-2237*

Local Stability and Hopf Threshold in a Lienard-Type Oscillator with Exponentially Filtered Feedback

Yosephus Decupertino Sumanto[1], Hafidh Khoerul Fata[1]

[1]Department of Mathematics, Faculty of Sciences and Mathematics, Universitas Diponegoro, Semarang, Indonesia.

Corresponding Author: Hafidh Khoerul Fata

DOI: https://doi.org/10.52403/ijrr.20260640

ABSTRACT

This study investigates the local stability and Hopf threshold of a three-dimensional Lienard-type oscillator with exponentially filtered feedback. The model couples a nonlinear second-order oscillator with a first-order filter variable so that the feedback acts through a smoothed memory of the main state. The equilibrium structure is characterized explicitly, and linearization at the origin is used to derive the characteristic polynomial. By applying the Routh-Hurwitz criterion, explicit algebraic conditions for local asymptotic stability are obtained. The equality case of the final Routh-Hurwitz inequality yields a Hopf threshold that separates stable equilibrium dynamics from oscillatory behavior. Numerical illustrations are proposed to visualize the stability regions, Hopf threshold curve, convergence to equilibrium, and sustained oscillations after the loss of stability. The results provide a compact analytical framework for understanding how nonlinear damping, feedback strength, and memory rate affect the dynamics of filtered-feedback oscillators.

Keywords: Lienard-type oscillator, filtered feedback, exponential memory, Routh-Hurwitz criterion, Hopf threshold, continuous dynamical system.

INTRODUCTION

Nonlinear oscillators represent a fundamental category of models within dynamical systems, as they offer straightforward mathematical depictions of self-sustained oscillations, damping mechanisms, and feedback-induced transitions. Within this category, Lienard-type systems hold significant importance due to their capacity to encapsulate nonlinear damping and restoring forces within a concise differential equation framework. Recent research on Lienard-type oscillators continues to underscore their significance in nonlinear mechanics, electrical circuits, and mathematical modeling, encompassing both analytical and computational analyses of nonlinear damping and oscillatory behavior. [1], [2], [3].

In numerous applications, the dynamics of an oscillator are influenced not solely by its current state but also by feedback signals and mechanisms akin to memory. Feedback can modify the stability of equilibrium, induce oscillatory behavior, or produce more complex dynamic responses. Controlled van der Pol-Duffing oscillators and delay-coupled nonlinear oscillators exemplify how feedback and coupling mechanisms can alter resonance, stability, and bifurcation structures. [4], [5]. In associated oscillator models, it has been demonstrated that non-viscous or exponential damping interacts

with nonlinearities, influencing both transient and long-term behaviors. [6].

Incorporating memory into a finite-dimensional continuous-time model can be achieved by introducing an auxiliary state variable regulated by a first-order filter. This variable does not function as an independent external force; instead, it offers an exponentially weighted depiction of the historical progression of the primary state variable. This method is conceptually linked to anticipatory dynamical systems, filtered feedback mechanisms, and memory-augmented oscillator models. [7], [8], [9], [10]. This observation aligns with recent advancements in memristor-based Lienard systems, where auxiliary variables incorporate memory effects, thereby enhancing the dynamic behavior of the oscillator. [11].

From an analytical standpoint, the initial step in comprehending such systems involves conducting a local stability analysis of their equilibria. In the context of three-dimensional ordinary differential equations, the characteristic polynomial of the linearized system is cubic. Consequently, the Routh-Hurwitz criterion offers a straightforward and effective method for determining whether all eigenvalues possess negative real parts. Related stability criteria, such as the Routh-Hurwitz and Lienard-Chipart type conditions, are standard tools in the analysis of oscillatory systems and feedback-controlled models.[12]. The crossing of the imaginary axis by a pair of complex conjugate eigenvalues is inherently linked to a Hopf threshold. This threshold represents a critical mechanism for the initiation of small amplitude oscillations.[13], [14], [15].

While the existing literature extensively explores nonlinear damping, feedback oscillators, memory-based systems, and Hopf bifurcation, there is a paucity of explicit low-dimensional models that integrate a Lienard-type nonlinear damping term with exponentially filtered feedback. Notably, a concise three-dimensional formulation that facilitates explicit equilibrium characterization, a closed-form Routh-Hurwitz stability condition, and a straightforward Hopf stability threshold could serve as a valuable foundation for further analytical and numerical studies. This gap has prompted the current investigation.

The objective of this study is to develop and examine a three-dimensional Lienard-type oscillator incorporating exponentially filtered feedback. The equilibrium structure is explicitly derived, and the local asymptotic stability of the non-degenerate equilibrium is assessed using the Routh-Hurwitz criterion. The derived Hopf threshold is presented in closed form, illustrating how the nonlinear damping parameter, feedback strength, and filtering rate collectively influence the stability boundary. Numerical simulations are employed to depict the stability regions, long-term amplitude variations, convergence to equilibrium, sustained oscillations, and the corresponding phase portrait. The structure of this paper is as follows: Section 2 introduces the model and its equilibrium structures; Section 3 details the linear stability analysis and Hopf threshold; Section 4 discusses the numerical stability regions and representative dynamics; and finally, Section 5 concludes the paper and suggests potential avenues for future research.

MODEL FORMULATION AND EQUILIBRIUM STRUCTURE

We consider a three-dimensional continuous-time system with exponentially filtered feedback. The model is given by the following system of equations:

$$\dot{x} = y, \quad \dot{y} = \alpha(1 - x^2)y - x + kz, \quad \dot{z} = \mu(x - z) \quad (1)$$

Here, $x(t)$ denotes the main state variable, $y(t)$ is its velocity-like component, and $\big(z(t)\big)$ is an auxiliary variable representing a filtered memory of $x(t)$. The parameter α controls the strength of the nonlinear damping term, k measures the feedback

strength from the memory variable to the main oscillator, and $\mu > 0$ is the filtering rate. A larger value of μ means that the memory variable $z(t)$ follows $x(t)$ more rapidly, while a smaller value of μ corresponds to a slower memory response.

The first two equations in system (1) form a Lienard-type oscillator. The additional variable $z(t)$ introduces a feedback signal generated from the past behavior of $x(t)$. This feedback is not introduced through an explicit time delay but through a first-order filtering equation. Solving the third equation of system (1) yields:

$$z(t) = e^{-\mu(t-t_0)}z(t_0) + \mu \int_{t_0}^{t} e^{-\mu(t-s)}\, x(s), ds \qquad (2)$$

Equation (2) shows that $z(t)$ is an exponentially weighted average of the previous values of $x(t)$, together with the contribution from the initial memory state $z(t_0)$. Hence, the model incorporates memory effects while remaining within the ordinary differential equation's framework. This formulation is useful because it allows the use of standard tools for finite-dimensional systems.

For compact notation, let $X = (x, y, z)^T$. Then system (1) can be written as follows.

$$\dot{X} = F(X)$$

Where

$$F(x, y, z) = \big(y, \alpha(1 - x^2)y - x + kz, \mu(x - z)\big)^T$$

An equilibrium point is a point $E = (x^*, y^*, z^*)$ *satisfying* $F(x^*, y^*, z^*) = 0$. From the first equation of system (1), we obtain $y^* = 0$. *From the third equation, since* $\mu > 0$*, we obtain* $z^* = x^*$. *Substituting* $y^* = 0$ and $z^* = x^*$ into the second equation gives

$$-x^* + kx^* = 0$$

or equivalently,

$$(k - 1)x^* = 0$$

Therefore, when $k \neq 1$, the system has a unique equilibrium point,

$$E_0 = (0,0,0)$$

The case $k = 1$ is degenerate. In this case, the equilibrium condition is satisfied for every real value of x^*, and the system has a continuum of equilibrium points given by

$$E_s = (s, 0, s), \quad s \in \mathbb{R}$$

Since the presence of a continuum of equilibria leads to a degenerate linearization problem, the subsequent analysis focuses on the nondegenerate case $k \neq 1$, where the origin E_0 is the unique equilibrium. The local stability of this equilibrium is investigated in the next section using the Jacobian matrix and the Routh-Hurwitz stability criterion.

LINEAR STABILITY AND HOPF THRESHOLD

In this section, we analyze the local stability of the nondegenerate equilibrium $E_0 = (0,0,0)$. The analysis is based on the linearization of system (1) around E_0. Because the vector field is smooth, the local behavior near equilibrium is determined by the eigenvalues of the Jacobian matrix, provided that no eigenvalue lies on the imaginary axis.

The Jacobian matrix of system (1) is

$$J(x, y, z) = \begin{pmatrix} 0 & 1 & 0 \\ -1 - 2\alpha xy & \alpha(1 - x^2) & k \\ \mu & 0 & -\mu \end{pmatrix}.$$

Evaluating this matrix at $E_0 = (0,0,0)$, we obtain

$$J_0 = \begin{pmatrix} 0 & 1 & 0 \\ -1 & \alpha & k \\ \mu & 0 & -\mu \end{pmatrix} \qquad (3)$$

The local stability of E_0 is determined by the roots of the characteristic equation $\det(\lambda I - J_0) = 0$. A direct computation gives

$$P(\lambda) = \lambda^3 + (\mu - \alpha)\lambda^2 + (1 - \alpha\mu)\lambda + \mu(1 - k). \qquad (4)$$

For convenience, we write (4) in the standard cubic form

$$P(\lambda) = \lambda^3 + a_1\lambda^2 + a_2\lambda + a_3,$$

Where

$$a_1 = \mu - \alpha, \qquad a_2 = 1 - \alpha\mu, \qquad a_3 = \mu(1 - k). \qquad (5)$$

By the Routh-Hurwitz criterion for a cubic polynomial, all roots of (4) have negative real parts if and only if

$$a_1 > 0, \qquad a_2 > 0, \qquad a_3 > 0, \qquad a_1 a_2 > a_3. \qquad (6)$$

Substituting the coefficients in (5) into (6), the equilibrium E_0 is locally asymptotically stable whenever

$$\mu - \alpha > 0, \qquad 1 - \alpha\mu > 0, \qquad \mu(1 - k) > 0,$$

and

$$(\mu - \alpha)(1 - \alpha\mu) > \mu(1 - k).$$

Since $\mu > 0$, the third inequality is equivalent to $k < 1$. Therefore, the stability conditions can be summarized as

$$\alpha < \mu, \qquad \alpha < \frac{1}{\mu}, \qquad k < 1,$$

and

$$(\mu - \alpha)(1 - \alpha\mu) > \mu(1 - k).$$

For fixed α and μ, the last inequality gives a lower stability threshold for the feedback parameter k. More precisely, the stable interval is

$$k_H < k < 1, \qquad k_H = 1 - \frac{(\mu - \alpha)(1 - \alpha\mu)}{\mu}. \qquad (7)$$

The value k_H is the linear Hopf threshold. On the boundary $k = k_H$, or equivalently $a_1 a_2 = a_3$, the characteristic polynomial can be factorized as

$$P(\lambda) = (\lambda + a_1)(\lambda^2 + a_2).$$

Hence, provided that $a_1 > 0$ and $a_2 > 0$, the eigenvalues on this boundary are

$$\lambda_{1,2} = \pm i\omega_H, \qquad \lambda_3 = -a_1,$$

Where,

$$\omega_H = \sqrt{a_2} = \sqrt{1 - \alpha\mu}. \qquad (8)$$

Thus, the curve defined by (7) represents the Hopf stability boundary for the linearized system. When the parameter k crosses this boundary, a pair of complex conjugate eigenvalues crosses the imaginary axis, while the third eigenvalue remains negative. The aforementioned result delineates the parameter values at which the equilibrium loses local asymptotic stability. Nevertheless, it does not ascertain the criticality of the Hopf bifurcation or the stability of the resultant periodic orbits. To obtain such information, a nonlinear normal form calculation or the computation of the first Lyapunov coefficient is necessary. This study confines its analytical approach to the Routh-Hurwitz stability condition and the associated Hopf threshold, while numerical simulations are employed to demonstrate the

transition from stable convergence to sustained oscillatory behavior.

NUMERICAL STABILITY REGIONS AND REPRESENTATIVE DYNAMICS

This section presents numerical illustrations of the analytical stability results obtained in the previous section. The purpose of the simulations was not to provide a complete nonlinear bifurcation analysis but to visualize the local stability region, Hopf stability threshold, and representative trajectories on both sides of the threshold. All simulations were performed for the Lienard-type filtered-feedback system defined in (1). Unless otherwise stated, the baseline parameters are $\alpha = 0.30$ and $\mu = 1.00$. For time-domain simulations, the initial condition is chosen as $(x(0), y(0), z(0)) = (0.20, 0, 0)$. The numerical integrations are carried out using a standard adaptive Runge-Kutta method with relative tolerance $1e-8$ and absolute tolerance $1e-10$. These values were sufficient to capture the qualitative transition from stable convergence to sustained oscillatory motion. The parameter values used in the numerical illustrations are listed in Table 1.

Table 1. Parameter settings used in the numerical experiments.

Numerical item	Fixed parameters	Varied parameter or condition
Stability map in (α, k)	$\mu = 1.00$	α and k varied
Stability map in (μ, k)	$\alpha = 0.30$	μ and k varied
Long-term amplitude diagram	$\alpha = 0.30, \mu = 1.00$	k varied
Stable time series	$\alpha = 0.30, \mu = 1.00$	$k = 0.80$
Oscillatory time series and phase portrait	$\alpha = 0.30, \mu = 1.00$	$k = 0.20$

Figure 1(a) shows the local stability region of the equilibrium E_0 in the (α, k)-plane for $\mu = 1.00$. The green region indicates the parameter values for which all characteristic roots have negative real parts, whereas the red region indicates the loss of local asymptotic stability. The black curve corresponds to the Hopf stability boundary predicted using the Routh-Hurwitz criterion. The figure shows that the feedback strength k cannot be chosen independently of the nonlinear damping parameter α. In particular, the stable region becomes narrower as α approaches the boundary values imposed by the inequalities in the linear stability condition.

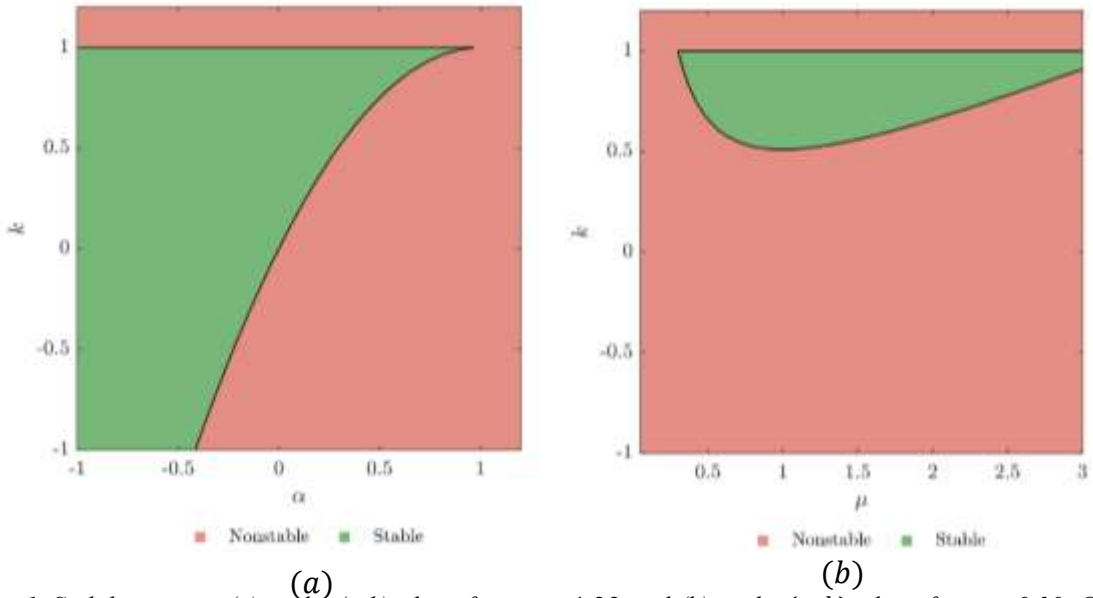

Figure 1. *Stability region (a) in the (α,k)-plane for $\mu = 1.00$ and (b) in the (μ, k)-plane for $\alpha = 0.30$. Green indicates local asymptotic stability of E_0, while red indicates loss of local stability. The black curve represents the boundary of Hopf stability.*

Figure 1(b) presents the corresponding stability region in the (μ, k)-plane for $\alpha = 0.30$. This plot illustrates the role of the filtering rate. When μ is small, the filtered variable $z(t)$ responds slowly to the main state $x(t)$, and the stability window in k is limited. As μ changes, the admissible range of k is modified by the Routh-Hurwitz conditions. This confirms that the memory filter is not merely an auxiliary equation but directly affects the local stability of the equilibrium.

To complement the two-parameter stability charts, Figure 2 shows a one-parameter numerical diagram obtained by varying k while keeping $\alpha = 0.30$ and $\mu = 1.00$ fixed. The diagram plots the long-term maximum and minimum values of $x(t)$ after transients. For k above the Hopf threshold and below $k = 1$, the trajectory converges to the equilibrium, so the long-term range collapses to zero. For k below the Hopf threshold, the equilibrium loses local stability and a sustained oscillatory response is observed. Therefore, this diagram provides a numerical illustration of the transition predicted by linear analysis.

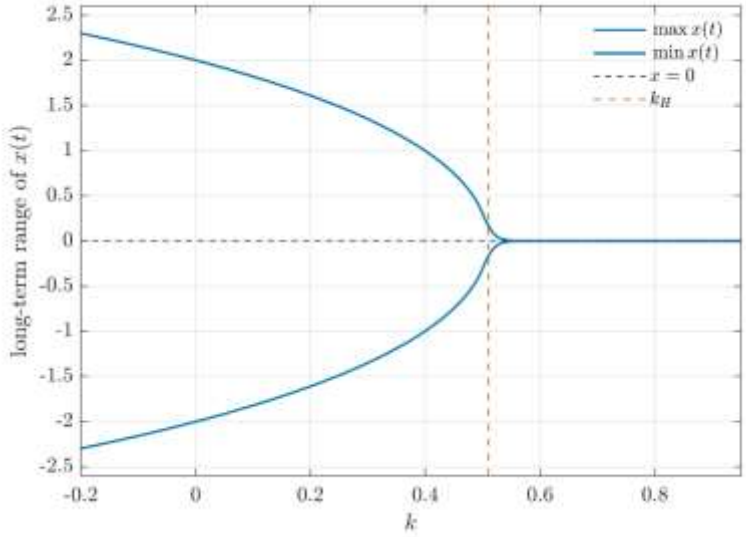

Figure 2. *Numerical long-term amplitude diagram with respect to k for $\alpha = 0.30$ and $\mu = 1.00$. The curves show the maximum and minimum values of $x(t)$ after transients. The dashed vertical line indicates the Hopf threshold kH predicted by the linear analysis.*

Figures 3 and 4 compare the representative trajectories on both sides of the Hopf stability threshold. Figure 3 corresponds to the stable regime with $k = 0.80$. In this case, the parameter value lies within the stability interval predicted by the Routh-Hurwitz criterion [16]. The variables $x(t), y(t)$, and $z(t)$ exhibit damped oscillations and converge to the equilibrium E_0. This behavior is consistent with the fact that all the eigenvalues of the linearized system have negative real parts.

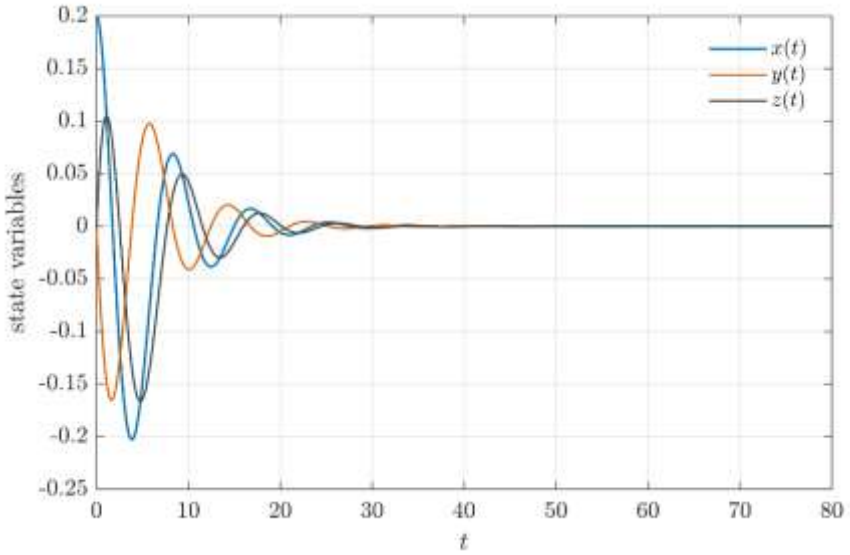

Figure 3. Time series for $\alpha = 0.30$, $\mu = 1.00$, and $k = 0.80$. All state variables converge to the equilibrium E_0.

In contrast, Figure 4 shows the response for $k = 0.20$, which lies outside the stable region for the same values of α and μ. Instead of decaying to zero, the solution exhibits sustained oscillations. The filtered variable $z(t)$ follows $x(t)$ with a smoother response, reflecting the memory-filtering mechanism in the third equation. This observation supports the interpretation that crossing the Hopf stability boundary leads to oscillatory dynamics.

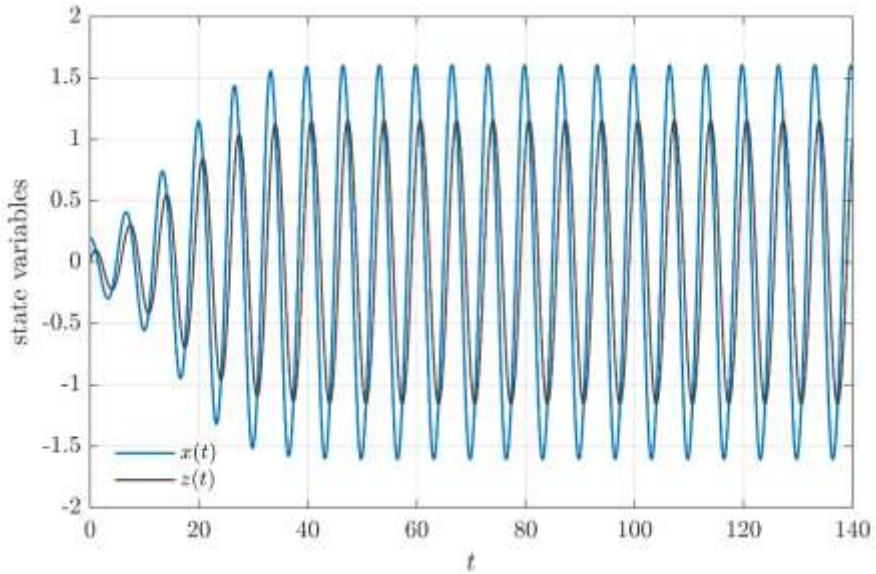

Figure 4. Oscillatory time series for $\alpha = 0.30, \mu = 1.00$, and $k = 0.20$. The filtered variable $z(t)$ follows $x(t)$ with a delayed and smoothed response.

The phase portrait in Figure 5 further illustrates this oscillatory regime. The trajectory in the (x, y)-plane approaches a closed curve surrounding the equilibrium E_0. This behavior was consistent with the sustained oscillations observed in the time series. However, the present analysis did not determine the criticality of the Hopf bifurcation. Establishing whether the Hopf bifurcation is supercritical or subcritical

requires a nonlinear normal form calculation or the computation of the first Lyapunov coefficient, which is beyond the scope of this study.

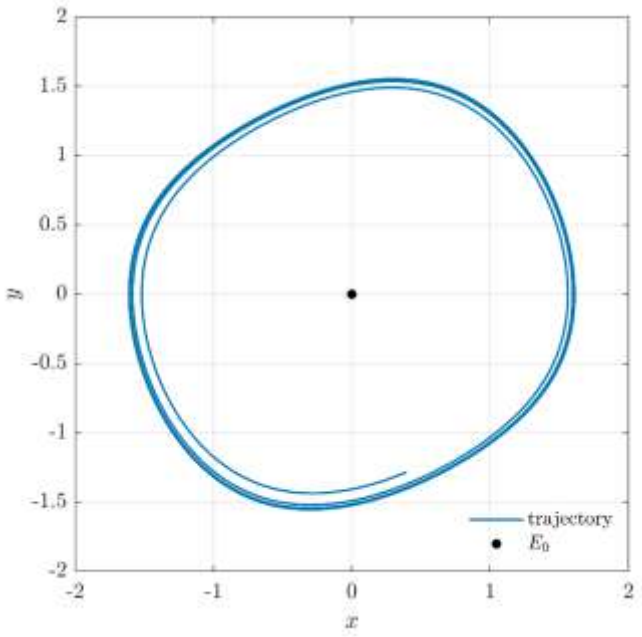

Figure 5. Phase portrait in the (x, y)-plane for the oscillatory regime with $\alpha = 0.30, \mu = 1.00$, and $k = 0.20$. The trajectory approaches a closed orbit surrounding E_0.

Overall, the numerical results were consistent with the analytical predictions. The stability maps show how the feedback strength and filtering rate shape the region of local asymptotic stability, whereas the time series and phase portrait illustrate the qualitative change from stable convergence to sustained oscillation after the loss of stability. These results provide a compact numerical confirmation of the Hopf stability threshold derived using the Routh-Hurwitz criterion.

CONCLUSION

In this study, a straightforward stability analysis of a Lienard-type oscillator with exponentially filtered feedback is presented. The model extends a classical nonlinear oscillator by incorporating a first-order memory variable, which represents an exponentially weighted response to the past behavior of the primary state variable. This formulation maintains the system within the framework of ordinary differential equations while integrating a memory-like feedback mechanism. The equilibrium structure reveals that, for the non-degenerate case where $k \neq 1$, the origin is the sole equilibrium of the system. The local stability of this equilibrium is analyzed using the Jacobian matrix and the Routh-Hurwitz criterion. The resulting stability conditions provide an explicit description of the stable parameter region in terms of the nonlinear damping parameter α, feedback strength (k), and filtering rate (μ). Notably, the analysis identifies a Hopf stability threshold that indicates the loss of local asymptotic stability at equilibrium.

The numerical simulations corroborate the analytical results. The stability regions in the selected parameter planes demonstrate how the feedback strength and filtering rate affect the stability of the equilibrium. The long-term amplitude diagram illustrates the transition from stable convergence to sustained oscillatory behavior as the feedback parameter is varied. Time series and phase portraits further confirm that, following the loss of local stability, trajectories may approach an oscillatory regime surrounding the equilibrium.

This study is intentionally confined to local stability and numerical illustrations. It does not ascertain the criticality of the Hopf bifurcation or establish the stability of the emerging periodic orbit through nonlinear normal form calculations. These issues may be addressed in future studies by computing the first Lyapunov coefficient, examining the global structure of periodic solutions, and investigating potential multistability induced by filtered feedback.

Declaration by Authors

Acknowledgement: None
Source of Funding: None
Conflict of Interest: No conflicts of interest declared.

REFERENCES

1. C. Ruby and M. Lakshmanan, "Liénard type nonlinear oscillators and quantum solvability," Phys. Scr., vol. 99, no. 6, p. 62004, 2024, doi: 10.1088/1402-4896/ad40dc.
2. F. Zadra, A. Bravetti, and M. Seri, "Geometric Numerical Integration of Liénard Systems via a Contact Hamiltonian Approach," 2021. doi: 10.3390/math9161960.
3. Gamal M Ismail and Galal M Moatimid, "Inspection of some nonlinear damped oscillators via the non-perturbative approach," J. Low Freq. Noise, Vib. Act. Control, vol. 45, no. 1, pp. 339–360, Mar. 2026, doi: 10.1177/14613484251382615.
4. J. C. Ji and N. Zhang, "Additive resonances of a controlled van der Pol–Duffing oscillator," J. Sound Vib., vol. 315, no. 1, pp. 22–33, 2008, doi: https://doi.org/10.1016/j.jsv.2008.01.052.
5. Z. Dadi, Z. Afsharnezhad, and N. Pariz, "Stability and bifurcation analysis in the delay-coupled nonlinear oscillators," Nonlinear Dyn., vol. 70, no. 1, pp. 155–169, 2012, doi: 10.1007/s11071-012-0438-7.
6. J. Sieber, D. J. Wagg, and S. Adhikari, "On the interaction of exponential non-viscous damping with symmetric nonlinearities," J. Sound Vib., vol. 314, no. 1, pp. 1–11, 2008, doi: https://doi.org/10.1016/j.jsv.2007.12.017.
7. Y.-J. Yang, C.-C. Chen, P.-Y. Lai, and C. K. Chan, "Adaptive synchronization and anticipatory dynamical systems," Phys. Rev. E, vol. 92, no. 3, p. 30701, Sep. 2015, doi: 10.1103/PhysRevE.92.030701.
8. C. McDonald and S. Yüksel, "Exponential filter stability via Dobrushin's coefficient," Electron. Commun. Probab., vol. 25, no. none, pp. 1–13, Jan. 2020, doi: 10.1214/20-ECP333.
9. V. S. Borges and M. Eisencraft, "A filtered Hénon map," Chaos, Solitons & Fractals, vol. 165, p. 112865, 2022, doi: https://doi.org/10.1016/j.chaos.2022.112865.
10. V. S. Borges, M. T. M. Silva, and M. Eisencraft, "Chaotic properties of an FIR filtered Hénon map," Commun. Nonlinear Sci. Numer. Simul., vol. 131, p. 107845, 2024, doi: https://doi.org/10.1016/j.cnsns.2024.107845.
11. S. L. Kingston and T. Kapitaniak, "Chapter 6 - Rich dynamics of memristor based Liénard systems," in Advances in Nonlinear Dynamics and Chaos (ANDC), C. Volos and V.-T. B. T.-M. for N. C. with A. I. A. Pham, Eds., Academic Press, 2021, pp. 125–145. doi: https://doi.org/10.1016/B978-0-12-821184-7.00014-1.
12. S. L. Wiggers and P. Pedersen, "Routh–Hurwitz-Liénard–Chipart Criteria BT - Structural Stability and Vibration: An Integrated Introduction by Analytical and Numerical Methods," S. L. Wiggers and P. Pedersen, Eds., Cham: Springer International Publishing, 2018, pp. 133–140. doi: 10.1007/978-3-319-72721-9_15.
13. H. K. Fata and N. Y. Ashar, "Bifurcations, Hidden Attractors, and Chaos in a Nonlinear Three-Dimensional System," Eur. J. Pure Appl. Math., vol. 18, no. 4, p. 6968, Nov. 2025, doi: 10.29020/nybg.ejpam.v18i4.6968.
14. M. HAN, J. YANG, and P. E. I. YU, "HOPF BIFURCATIONS FOR NEAR-HAMILTONIAN SYSTEMS," Int. J. Bifurc. Chaos, vol. 19, no. 12, pp. 4117–

4130, Dec. 2009, doi: 10.1142/S0218127409025250.
15. H. Natiq, M. R. Said, N. M. G. Al-Saidi, and A. Kilicman, "Dynamics and Complexity of a New 4D Chaotic Laser System," 2019. doi: 10.3390/e21010034.
16. T. S. Amer, A. I. Ismail, M. O. Shaker, W. S. Amer, and H. A. Dahab, "Stability and analysis of the vibrating motion of a four degrees-of-freedom dynamical system near resonance," J. Low Freq. Noise, Vib. Act. Control, vol. 43, no. 2, pp. 765–795, Jan. 2024, doi: 10.1177/14613484231221483.

How to cite this article: Yosephus Decupertino Sumanto, Hafidh Khoerul Fata. Local stability and Hopf threshold in a Lienard-type oscillator with exponentially filtered feedback. *International Journal of Research and Review*. 2026; 13(6): 409-418. DOI: *https://doi.org/10.52403/ijrr.20260640*

******